
MATHEMATICAL MODELING
IN NUCLEAR TECHNOLOGIES

Updated Model for Thermal Conductivity Calculation of Thin Films of Silicon and Germanium

A. A. Barinov^{a,*}, B. Liu^a, V. I. Khvesyuk^a, and K. Zhang^a

^a*Bauman Moscow State Technical University, Moscow, 105005 Russia*

**e-mail: barinov@bmstu.ru*

Received October 18, 2018; revised December 24, 2018; accepted February 15, 2019

Abstract—A model for calculation of thermal conductivity of thin films of silicon and germanium is presented on the basis of solving the Boltzmann equation in the time relaxation approximation. The unique feature of this model is the application of recent achievements in determination of the time of phonon–phonon interactions obtained from “first principles” and also the use of real dispersion curves and the propagation velocities of phonons with different polarization. The proposed approach contains no averaging and fitting parameters, which already for more than half a century and until now have been common in calculations of thermal conductivity of macroscopic bodies and nanostructures. A detailed qualitative and quantitative comparison of results of calculations by the “classical” and “updated” models is carried out. Problems in the methods for calculating thermal conductivity for simulation of new structures in advanced semiconductor devices and ways of their further development are set forth.

Keywords: thermal conductivity, nanofilms, size effect

DOI: 10.1134/S1063778820100038

INTRODUCTION

For the past decade, a tremendous growth of technologies based on using structures of micro- and nanoscales is observed. For example, a typical scale of hardware components—transistors—already has reached 10 nm. The tendency toward a reduction in size of components, in the first place, leads to a drop of thermal conductivity by several orders of magnitude owing to the so-called size effect [1], which is the exceptional property of micro- and nanomaterials. In the second place, this generates the awesome growth of heat release: the magnitude of heat flow in electronic devices already reaches 100 W/cm² [2]. Since the workability of microelectronic devices strongly depends on temperature, a problem of ensuring the necessary thermal regime arises, which requires searching for ways of heat removal. The presented arguments testify to the necessity of studying the thermal properties of objects based on micro- and nanostructures [3].

A distinctive feature of processes in nanostructures are, firstly, inapplicability of classical transport laws (e.g., for heat transfer, the Fourier law) and, secondly, a strong dependence of properties on geometry and shape of the sample [4]. Therefore, despite the variety of well-known methods for determination of macroscopic object properties, many unsolved problems remain in the area of micro- and nanoscales, which require combining efforts of research groups on the

world scale. There is as yet no unambiguous answer to the question about the heat transfer calculation and even more about the simulation of devices based on micro- and nanostructures. The search for a solution to this problem remains open.

In this work, the process of heat transfer in the longitudinal direction in films of silicon and germanium for the thickness range from 100 μm to 10 nm is studied. This is connected, firstly, with a wide occurrence of these components in semiconductor electronics, and, consequently, with the need for methods having a sufficiently strong predictive ability. Secondly, this provides the possibility to compare the calculation results with the available experimental data. In [5], it is possible to become familiar with the calculation of thermal conductivity in the transverse direction.

At present, the widespread method of thermal conductivity calculation is based on solving the Boltzmann equation using a relaxation time approximation. Therefore, the main task is to find such relations and coefficients for the time of phonon–phonon interactions which would allow to construct an approximating function for thermal conductivity compliant with experimental data. In this case, the coefficients found as a result of fitting are not universal, since they are strongly tied to the accepted assumptions, do not indicate the physics of interaction processes, and restrict the application of the method. Moreover, the problem of calculating the thermal conductivity of films is a

multiparametric one, which does not allow to use general method for bulk and requires searching for a new approach to the calculation and prediction of properties of micro- and nanoscale structures.

The goal of this work is to construct a generalized model in which, firstly, there is no need for simplifications and fitting parameters, which are commonly used in the calculations, and, secondly, which would allow estimations (predictions, as is said in the foreign literature) of thermal conductivity values of films within a wide range of thicknesses and temperatures. To solve the stated problem, strict expressions for dispersion curves and relations for the time of interaction of phonons with each other are applied on the basis of modern strict models “from the first principles” [6].

1. CONSTRUCTION OF MODEL FOR THERMAL CONDUCTIVITY CALCULATION OF FILMS

1.1. Basics of Thermal Conductivity Calculation

Heat carriers in semiconductors and dielectrics are the phonon quasiparticles—quanta of elastic waves propagating in solid bodies [7]. Each phonon can be involved in the following interaction processes. In the first place, there is the interaction of phonons with each other, among which the main role is played by the processes with involvement of three phonons. The phonon–phonon interactions are possible either with momentum conservation (normal processes) or with momentum transfer to the crystalline lattice (Umklapp scattering). In the second place, there are processes of phonon scattering on isotopes, dislocations, and impurities (lattice irregularities). In the third place, there is the interaction with boundaries of the sample. In this case, in contrast to bulk materials, where the size effect is dominant only at temperatures below 10–20 K, in micro- and nanostructures, this process depending on the characteristic sample size has a considerable influence up to the Debye temperature and higher.

The description of the phonon gas state is based on solving the Boltzmann transfer equation for phonons in the relaxation time approximation

$$\mathbf{v} \cdot \nabla T \frac{\partial f}{\partial T} = \frac{f - f_0}{\tau}. \quad (1)$$

Here \mathbf{v} is the phonon velocity, m/s, equal to the group velocity of the elastic wave: $\mathbf{v} = \partial\omega/\partial\mathbf{k}$, where ω is the wave frequency, s^{-1} , and \mathbf{k} is the wavevector, m^{-1} ; T is the temperature of the solid body, K; f is the sought nonequilibrium function of phonon distribution over energies; f_0 is the equilibrium Bose–Einstein function; τ is the relaxation time of phonon gas, s.

It should be noted that, in materials with the diamond-like crystalline lattice (silicon, germanium, diamond), the phonon gas consists of acoustic and optical phonons of longitudinal and transverse polar-

izations. Owing to small velocities of propagation, optical phonons are not taken into account, but their involvement in the interaction process cannot be neglected. More details about the specific features of optical waves in the lattice can be found in article [8]. Therefore, this work considers acoustic phonons of three polarizations: longitudinal LA and two transverse TA.

From solving Eq. (1), the equation for thermal conductivity calculation can be obtained

$$\kappa(T) = \frac{1}{3} \sum_j \int_0^{\omega_{\max,j}} C_{ph}(\omega, T) D_j(\omega) v_{g,j}(\omega) l_j(\omega, T) d\omega, \quad (2)$$

where the summation is performed over the polarizations j , $C_{ph}(\omega, T) = \hbar\omega \frac{df_0(\omega, T)}{dT}$ is the phonon specific heat, $D_j(\omega) = \frac{1}{2\pi^2} \frac{\omega^2}{v_{g,j}(\omega)v_{p,j}^2(\omega)}$ is the density of state (DOS), $l_j(\omega, T) = v_{g,j}(\omega)\tau_j(\omega, T)$ is the mean free path of the phonon, $v_{g,j}(\omega) = d\omega/dk$ is the group velocity of the phonon, $v_{p,j}(\omega) = \omega/k$ is the phase velocity of the phonon, and $\omega = f_j(k)$ is the dispersion relation. Here and below, we consider the quasi-isotropic approximation and properties in the direction [100] of the crystalline lattice, along which the transverse waves are degenerate (branches coincide TA1 = TA2 = TA).

From the analysis of Eq. (2), it can be seen that, for the thermal conductivity calculation of semiconductors and dielectrics, it is necessary to know two underlying quantities.

Firstly, the dependence of the group $v_{g,j}$ and phase $v_{p,j}$ velocities on the frequency is required. For this purpose, it is necessary to analyze the crystalline lattice dynamics and to derive the dispersion relations $\omega = f(k)$. This is the first fundamental component in considering processes of phonon propagation inside structures of any scale (macro-, micro-, and nanoscale).

Secondly, the times of phonon interactions are necessary for different processes inside the crystalline lattice, namely: τ_{ph-ph} is the time of phonon–phonon interactions, τ_{imp} is the time of phonon scattering on the lattice impurities, and τ_B is the time of phonon interaction with the lattice boundaries. Since each scattering process is independent, the total time of scattering τ_j for each polarization j is defined according to the Matthiessen’s rule:

$$\tau_j^{-1} = \tau_{ph-ph,j}^{-1} + \tau_{imp,j}^{-1} + \tau_{B,j}^{-1}. \quad (3)$$

Consequently, for the thermal conductivity calculation of a solid body, firstly, dispersion relations $\omega = f(k)$ and, secondly, times of phonon scattering

for different interaction processes in the crystalline lattice are required.

1.2. Classical Models of Determination of Dispersion Relations and Time of Different Phonon Interaction Processes

At the present time, the most commonly known model is the model proposed in 1963 [9] by Holland, which is based on the following assumptions. In the first place, the real law of dispersion $\omega(k)$ is replaced by the bilinear approximation

$$\omega_{TA} = \begin{cases} v_{T0}k, & \omega < \omega_{T1} \\ v_{TU}k, & \omega_{T1} < \omega < \omega_{TA,max} \end{cases} \quad (4)$$

$$\omega_{LA} = \begin{cases} v_Lk, & \omega < \omega_{L1} \\ v_{L1}k, & \omega_{L1} < \omega < \omega_{LA,max}, \end{cases}$$

i.e., each branch (LA and TA) is divided into two segments on which the velocity is constant. In the second place, expressions for phonon–phonon interactions are reduced to the consideration of segments on each there is its own interaction process:

$$\tau_{ph-ph}^{-1} = \begin{cases} \tau_{T,N}^{-1} = B_T \omega T^4, & \omega < \omega_{TA,1/2} \\ \tau_{T,U}^{-1} = B_{TU} \omega^2 / \sinh(x) \\ \omega_{TA,1/2} < \omega < \omega_{TA,max} \\ \tau_L^{-1} = B_L \omega^2 T^3, & 0 < \omega < \omega_{LA,max}. \end{cases} \quad (5)$$

In this case, the coefficients B_T , B_{TU} , and B_L in Eq. (5) are used for fitting the value of thermal conductivity (2) to experimental data. Moreover, when instead of bilinear approximation (4) other dependences of $\omega(k)$ are used, the thermal conductivity value strongly differs from the original (by several times); see [10]. This is evidence that times of phonon–phonon interactions (5) do not reflect the real scattering process, while they only serve for fitting to experimental data and cannot be used beyond the initial model.

The similar situation is with the Slack model [11, 12], which is based on the replacement of real dispersion laws by linear ones (with a constant rate), while taking into account the phonon–phonon interactions consists of two Umklapp processes according to the relations

$$\tau_{ph-ph}^{-1} = \begin{cases} \tau_{T,U}^{-1} = B_{TU} \omega^2 T \exp(-\theta_T/3T) \\ \tau_{L,U}^{-1} = B_{LU} \omega^2 T \exp(-\theta_L/3T) \end{cases} \quad (6)$$

and normal processes, which in [12] coincide with expressions from the Holland model [9]. In this case, coefficients B_{TU} , B_{LU} (and analogous B_{TN} , B_{LN}), contain the possibility to adjust the obtained solution to the experimental data by varying Grüneisen parameters for the transverse and longitudinal polarizations.

Time of scattering on crystalline lattice impurities.

Currently in the overwhelming number of calculations, the analysis of the scattering processes on impurities (including isotopes) is based on the relation obtained by Klemens in 1955 [13]:

$$\tau_{imp}^{-1} = A\omega^4, \quad (7)$$

in which A is a constant depending only on the concentration of impurity atoms and isotopes in the materials. It is assumed that the material is isotropic and the phonon propagation velocity is equal to the average Debye velocity $v_S^{-3} = 1/3(v_L^{-3} + 2v_T^{-3})$, where v_L and v_T are the propagation velocities of elastic waves in the macroscopic sample.

Using Eq. (7) in thermal conductivity calculations assumes that the real dispersion of phonons is ignored. Consequently, this leads to erroneous calculations within the ranges of temperatures and film thicknesses where the influence of scattering on impurities is dominant. A stricter analysis of scattering processes was carried out by Tamura [14], and the expression appears as follows:

$$\tau_{imp,j}^{-1} = \frac{\pi}{6} V_0 g \omega^2 D_j(\omega), \quad (8)$$

where V_0 is the crystalline lattice volume per one atom; g is the parameter corresponding to the content of impurity atoms in the lattice, $g = \sum_i f_i (\Delta M_i / M)^2$; and f_i is the concentration of the i th isotope, the mass of which differs from the average M by the quantity ΔM_i .

In [14], it is shown that the calculation by Eq. (7) gives a result overstated by several times as compared to Eq. (8) in the range of frequencies close to ω_j^{max} . In other words, at temperatures on the order of and higher than the Debye temperature, where the influence of high-frequency phonons is great, the value of thermal conductivity is overstated knowingly. Thus, the necessity of application of fitting parameters is created artificially.

Time between consecutive interactions with a boundary. Taking into account processes of phonon scattering on the sample boundary is the weakest point of the existing theories, especially in calculations of thermal conductivity of micro- and nanostructures. The time τ_B until now in the overwhelming majority of works has been determined according to the simple Casimir–Ziman relation [15, 16]

$$\tau_B^{-1} = v_S / L_e, \quad (9)$$

where L_e is the effective length, $L_e = L(1-p)/(1+p)$; L is the characteristic size of the sample, $L = 2/\pi^{1/2} (a \times b)^{1/2}$; $a \times b$ is the cross section of the sample; and p is the specular reflection parameter.

Table 1. Coefficients for time of phonon–phonon interactions [17]

	A_{TA}^N , (meV ² K s) ⁻¹	A_{LA}^N , (meV ² K s) ⁻¹	A_{TA}^U , (meV ⁴ K s) ⁻¹	A_{LA}^U , (meV ⁴ K s) ⁻¹	θ_D , K
Si	253322	163921	2012	507	658
Ge	460248	401980	8634	1990	376

The parameter p takes into account the probability that a phonon in the interaction with a real (rough) surface scatters specularly: $p = 1$ corresponds to specular reflection; $p = 0$ corresponds to diffuse reflection.

The value of specular reflection parameter p depends on the relation between the mean square roughness of the sample surface δ and the wavelength of the incoming phonon λ . So, the phonons for which $\lambda \gg \delta$ scatter specularly, while at $\lambda \ll \delta$, they scatter diffusively. At the moment, a unique formula showing this interrelation is the Ziman formula according to which the value of the specular reflection parameter can be derived from the Gaussian distribution:

$$p = \exp(-16\pi^3\delta^2/\lambda^2). \quad (10)$$

The application of Eq. (10) for phonons is erroneous, since, firstly, this expression is valid only for electromagnetic waves; secondly, an incident wave is oriented along the normal to the surface; and, thirdly, the decay processes of acoustic waves after reflection on the boundary are ignored. Consequently, at the present time, there is no expression for calculating the probability of specular reflection for acoustic waves incident on the surface at different angles. Therefore, the parameter p in Eq. (9) is accepted as the average value and is used for fitting the results of the thermal conductivity calculation to experimental data.

It should also be stressed that Eq. (9) ignores the relation between the free path length of phonons in the macroscopic sample l_∞ and the characteristic size of the structure under consideration L (thickness for films), which represents the Knudsen number $Kn = l_\infty/L$ —the most important characteristic determining the regime of heat propagation in the solid body. So, at $Kn \gg 1$, the regime is diffusive; i.e., the classical Fourier law of thermal conductivity is valid; at $Kn \ll 1$, the regime is ballistic; the processes of phonon interaction with the walls dominate; at values of $Kn \approx 1$, the regime is diffusion-ballistic and occupies the intermediate region.

The presented specific features of the widely applied models based on using fitting parameters lead to the necessity of searching for modern methods of calculation of the dispersion relations and times of phonon interaction.

1.3. Updated Model of Thermal Conductivity Calculation

The present level of development of computational technology makes it possible, in the first place, to use the modern methods of calculation of times of phonon–phonon interactions from “first principles” [6], which contain no fitting parameters and reflect the “physics” of the process better than models described in section 1.2. In the second place, the possibility appears for constructing and taking into account the real dispersion of phonons instead of models with constant velocity: single-speed approach of Debye and bilinear approximation of Holland (4).

Times of phonon–phonon interactions. In this work, the phonon–phonon times for the normal and Umklapp processes are used, which were derived by Ward and Broido [17] on the basis of analysis of phonon interaction processes from the “first principles”:

$$\begin{aligned} \tau_{ph-ph,j}^{-1}(\omega, T) &= \tau_{N,j}^{-1} + \tau_{U,j}^{-1} \\ &= A_j^N \omega^2 Tf(T) + A_j^U \omega^4 Tf(T), \end{aligned} \quad (11)$$

where $f(T) = 1 - \exp(-3T/\theta_D)$, and j is the transverse TA and longitudinal LA polarizations. Values of coefficients are presented in Table 1.

Despite the clear superiority of Eq. (11) (absence of fitting parameters and a direct connection with simulation of processes of three-phonon interactions), it has not found widespread occurrence in calculations until now.

Figure 1 presents a comparison of times of phonon–phonon interactions according to models of Holland (5), Slack (6), and Ward–Broido (11) for silicon at a temperature of 300 K. It can be seen on the plots that the calculation results for these three models agree only at low frequencies and diverge with growth in phonon energy; here it can be noted that the Holland model overestimates the contribution of phonons of transverse polarization.

Time of scattering on boundaries. Taking into account the phonon interaction with sample boundaries is the cornerstone in thermal conductivity calculation of nanostructures. Now there is no strict method for the analysis of phonon scattering on the boundary. One of the possible ways for solving this problem may be calculations based on the Monte Carlo method. The further prospects in this direction can be found in [18]. In this work, the calculation of time of scattering on film boundaries is based on Eq. (9) with the use of the real dispersion law.

Construction of real dispersion curves. To determine the dispersion curves, the lattice dynamics method (LDM) is used at the present time [6], which allows to derive the dependence $\omega(k)$ in main crystallographic directions. The method provides a good agreement with the results of experiment, but requires significant computational efforts and certain skills in mastering the LDM. This work applies the method for

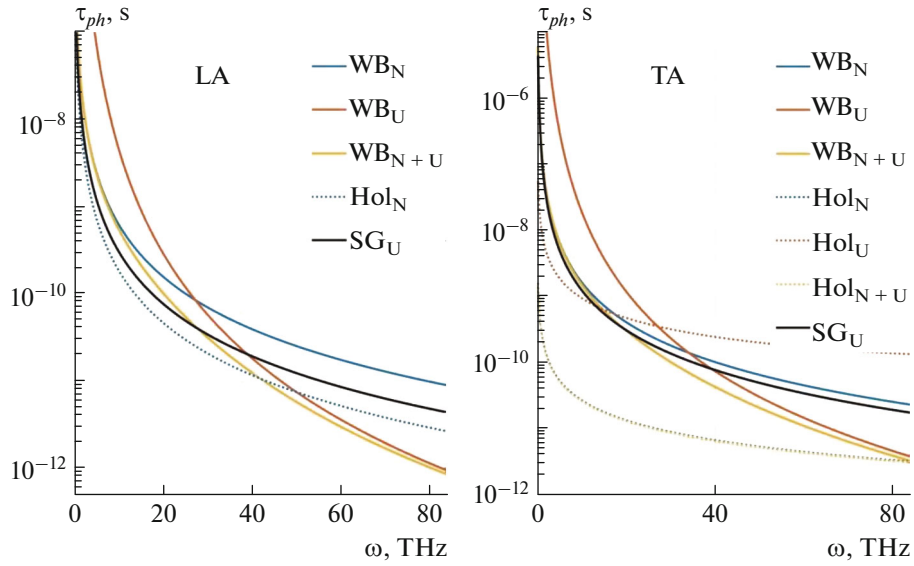


Fig. 1. Times of phonon–phonon interactions: WB is the Ward–Broido model (11), Hol is the Holland model (5), and SG is the Slack model (6); indices correspond to the process type: N is the normal processes, U is the Umklapp processes.

approximating experimental data by polynomial relations, which allows to substantially simplify the calculations.

The tables of experimental data on $\omega(k)$ for silicon and germanium [19, 20] serve as initial data for approximation. As reference (definitive) points, the following values are used:

$$\begin{cases} k_j = 0, & \omega_j = 0 \\ k_j = 0, & v_{g,j} = v_{g0,j} \\ k_j = \pi/a, & \omega_j = \omega_{\max,j} \\ k_j = \pi/(2a), & \omega_j = \min(\Delta\omega_{\max,j}) \\ + k_{TA} = \pi/a, & v_{TA} = 0. \end{cases} \quad (12)$$

Thus, for a longitudinal wave, we derive four conditions and the cubic polynomial, while for a transverse wave, we obtain five conditions and the quartic polynomial; the analytical dependence for the dispersion relation takes the form

$$\omega_j = \sum_{n=0}^{N_j} c_n k^n, \quad (13)$$

where $N_{TA} = 3$ and $N_{LA} = 2$. With substitution of Eq. (13) to system (12), we derive a system of linear algebraic equations for finding the polynomial coefficients c_n . The results of calculation of the c_n values of the approximating polynomial for dispersion relations of silicon and germanium in the direction [100] of the crystalline lattice are given in Table 2.

Figure 2 presents the dispersion relations for silicon along the direction [100] of the crystalline lattice, which are compared with experimental data and the Holland bilinear model.

Other variants of approximation dependences for the phonon dispersion are also known, the analysis of which is presented in [10]. A distinctive feature of the method (Eqs. (12), (13)) proposed by the authors of the work is the employment of reference points not only at the center and on the boundary of Brillouin zone but also at an intermediate point, which makes it possible to take into account the behavior of real dispersion curves inside the Brillouin zone and, as a consequence, to obtain the best agreement with experimental data (see Fig. 3).

The presented model of phonon–phonon interactions of Ward–Broido [17] and the method for taking into account the real phonon dispersion make it possible to exclude fitting parameters, associated with many simplifications and uncertainties, included in the commonly used and widespread models of thermal conductivity calculation of silicon, germanium, and other semiconductor materials.

2. CALCULATION RESULTS

2.1. Calculation of Thermal Conductivity of Macroscopic Samples

To check the accuracy of the updated model, the thermal conductivity is calculated for a sample of germanium with the natural content of isotopes (Fig. 4) and silicon (Fig. 5). The calculation results are compared with the known experimental data [21, 22].

Figure 4 provides insight into the dependence of thermal conductivity on temperature of semiconductor materials. As can be seen from the comparison of different approximating dependences for the dispersion relations, the error in determination of thermal

Table 2. Values of coefficients of approximating polynomial $\omega(k)$ (13)

$k, 1/\text{m}$ $\omega, 1/\text{s}$	$\bar{\omega}_j(x) = c_4x^4 + c_3x^3 + c_2x^2 + c_1x + c_0, \bar{\omega} = \omega/10^{13}, x = k/k_{\text{max}}$				
Coefficients for silicon Si	c_0	c_1	c_2	c_3	c_4
$j = \text{TA}$	0	6.759	-3.353	-2.288	1.702
$j = \text{LA}$	0	9.756	-0.371	-1.644	0
$j = \text{TO}$	9.758	0	-5.967	7.837	-2.894
$j = \text{LO}$	9.770	0	-1.220	-8.091	0
Coefficients for germanium Ge	c_0	c_1	c_2	c_3	c_4
$j = \text{TA}$	0	3.930	-2.705	-0.323	0.612
$j = \text{LA}$	0	5.459	0.052	-0.982	0
$j = \text{TO}$	5.730	0	-4.200	6.240	-2.580
$j = \text{LO}$	5.743	0	-0.496	-0.716	0

conductivity lies within the limits of 10–15%. The analysis of the presented approximations makes it possible to explicitly distinguish a number of regions: the temperature range much below the Debye temperature, where the processes of scattering on sample boundaries (below 10 K) and on isotopes (from 10 to 50 K) play the defining role, and the temperature range on the order of the Debye temperature and higher, where the main role is played by the processes of phonon–phonon interactions (more than 50 K).

For investigation of thermal conductivity at the Debye temperature and higher, we consider the silicon sample with the natural content of impurity atoms from [22] and compare with experimental data [22].

The calculation results presented in Fig. 5 show the fundamental specific feature of the Holland model: reassessment of a role of transverse waves in processes of phonon–phonon interactions. This circumstance does not lead to an error in the determination of thermal conductivity, but underestimates the contribution of longitudinal waves. This is one of negative aspects of the fitting nature of the Holland model, which gives no way for the adequate estimation of the contribution from the individual waves, and also creates a false impression about the applicability of the model to the calculation of any semiconductor structures (from macro to micro and nano).

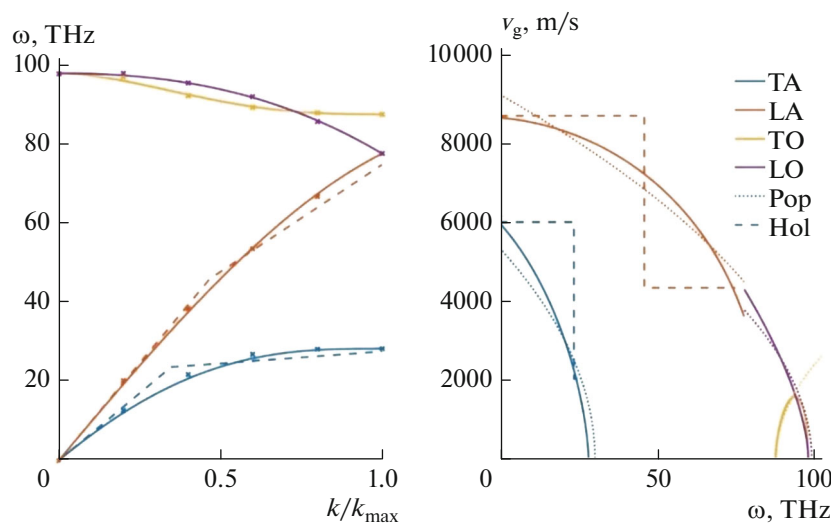


Fig. 2. Dispersion curves and group velocities of silicon for the direction [100]. TA and LA are the transverse and longitudinal acoustic waves; TO and LO are the transverse and longitudinal optical waves. Dots indicate the experimental data [19], solid lines show the approximation of the authors (13), dashed “Hol” indicates the Holland approximation (4), and “Pop” is the work [10].

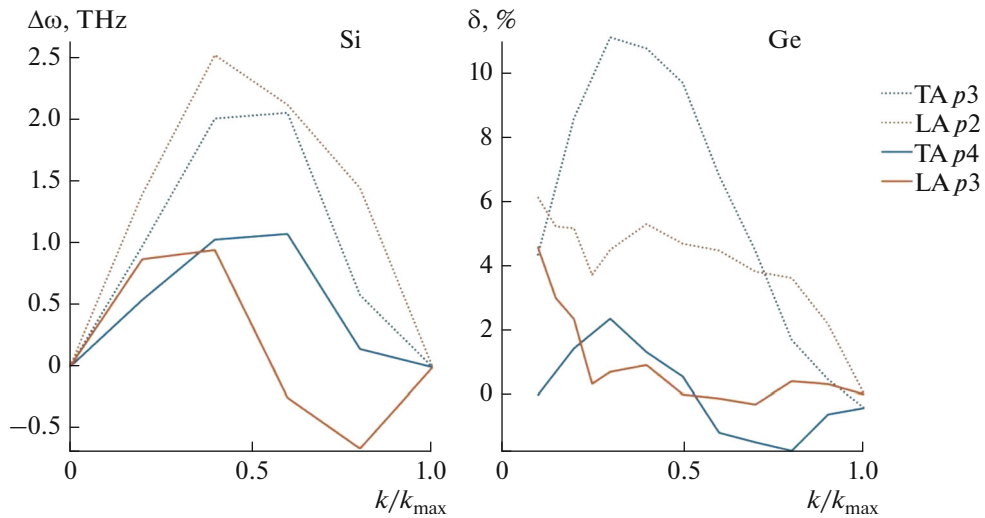


Fig. 3. Error of calculation of dispersion relations for silicon and germanium in comparison with experimental data [19, 20]: solid lines refer to the model of the authors, dotted lines correspond to the model of the lower order [10, 21], and p corresponds to the order of the approximating polynomial (13).

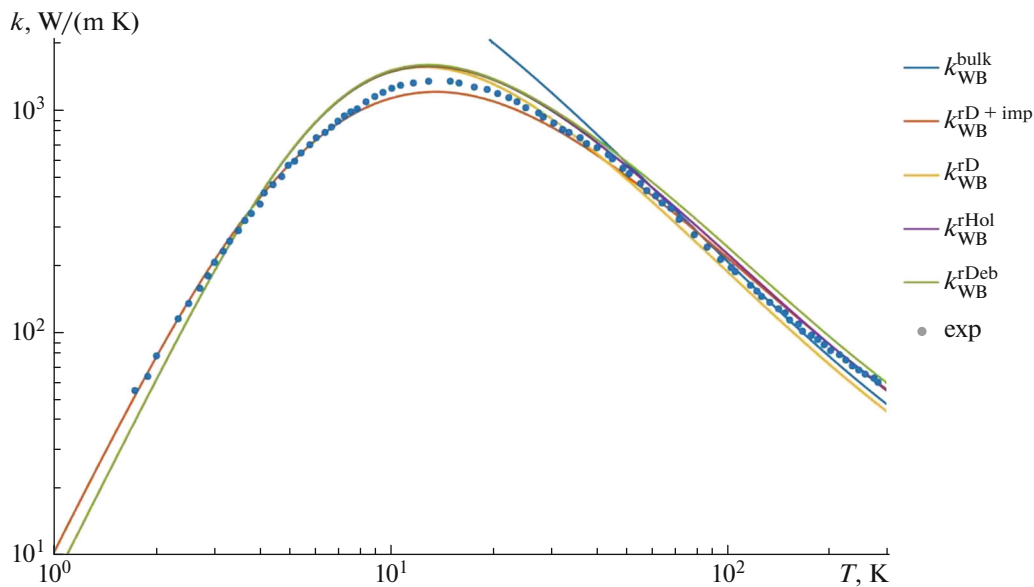


Fig. 4. Thermal conductivity of germanium with the natural content of isotopes (36.5% ^{74}Ge + 27.4% ^{72}Ge + 20.5% ^{70}Ge + 7.8% ^{73}Ge + 7.8% ^{76}Ge). $k_{\text{WB}}^{\text{bulk}}$ denotes that the calculation is performed using the phonon–phonon times of interaction according to the Ward–Broido model. $k_{\text{WB}}^{\text{rD+imp}}$ denotes the same taking into account the real phonon dispersion in the calculation of scattering on isotopes by Eq. (8). Further, the results are presented taking into account the scattering on impurities (7) and on sample boundaries with allowance for the following dispersion laws: $k_{\text{WB}}^{\text{rD}}$ is the approximation of real dispersion relations (12), (13); $k_{\text{WB}}^{\text{rHol}}$ is the bilinear Holland model (4); $k_{\text{WB}}^{\text{rDeb}}$ is the model with constant velocity. Dots correspond to the experimental data from [21].

2.2. Calculation of Thermal Conductivity of Films

For the accuracy check of the updated model and demonstration of the influence of the size effect, the thermal conductivity calculation of silicon films is performed within a thickness range from 10 nm to 100 μm

and a temperature range from 20 to 450 K. The results are compared with the known experimental data [23–26].

Figure 6 presents a typical dependence of the thermal conductivity of semiconductor materials on the

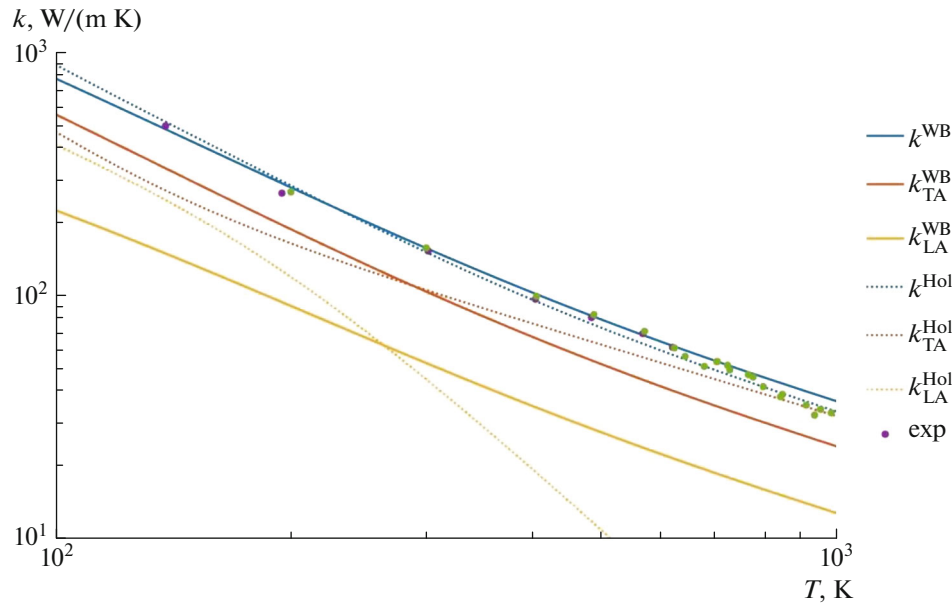


Fig. 5. Thermal conductivity of silicon: comparison of the model of the authors k^{WB} and the Holland model k^{Hol} (4), (5) with the experimental data [22] (dots). Indices correspond to polarization: LA means longitudinal, TA means transverse.

film thickness by an example of silicon along the direction [100]. From the analysis of the plots, the conclusion can be drawn that the employment of the Holland model leads, firstly, to a significant uncertainty in the results, since the possibility appears by means of the parameter of specular reflection to vary freely the value of thermal conductivity within wide limits (from the minimum presented in the figure to 1), which allows the obtained results to be fitted to any experimental data. The application of the authors' model makes it possible to localize a region of the possible value of thermal conductivity and to derive more accurate estimates. Secondly, the slope ratio of thermal conductivity in the Holland model differs from the estimates of more accurate models (the model of the author and the Asheghi model [23]) and experimental data [23], which indicates the clear superiority of taking into account the real dispersion relations and times of phonon–phonon interactions from "first principles" without introducing fitting parameters.

Similar conclusions can be drawn from the analysis of the thermal conductivity of silicon as a function of temperature for different film thicknesses, which is presented in Fig. 7.

Figure 8 shows a difference between the thermal conductivity of films k_{Hol} calculated from the Holland model and the thermal conductivity k derived using the updated model: $\text{mismatch} = (k - k_{\text{Hol}})/k \times 100\%$. It can be seen that the error in the thermal conductivity determination strongly depends on the temperature and thickness of films and may reach 120%. Therefore the application of models based on simplifications and

fitting parameters leads to an uncontrolled behavior of the result.

For demonstration of the phonon dispersion influence on the thermal conductivity calculation, Fig. 9 shows the comparison of the thermal conductivity using the linear law with the one using the polynomial law (Eq. (10)). When considering the thermal conductivity of structures in which the size effect takes place, it can be seen that the application of linear dispersion laws leads to a significant underestimation of the contribution from the real dispersion law to the phonon propagation processes. This leads to the necessity of introducing additional fitting parameters which brings even greater uncertainty into the estimation of thermal conductivity of micro- and nanostructures.

It turns out that now there are many models for the thermal conductivity calculation of semiconductor structures of the micro- and nanoscale, which contain a great number of fitting parameters. This circumstance introduces a significant uncertainty into the thermal conductivity calculation and does not allow the adequate estimation of properties of the structures in which the size effect takes place. To solve the stated problem, the authors have involved modern methods of calculation based on minimizing the number of adjustable parameters. This allowed, firstly, to minimize the uncertainty in the thermal conductivity calculation due to the detailed description of phonon propagation processes. Secondly, the factor limiting the further improvement of the accuracy of thermal conductivity estimation was established: the absence of an adequate model of calculation of the time of scattering on boundaries.

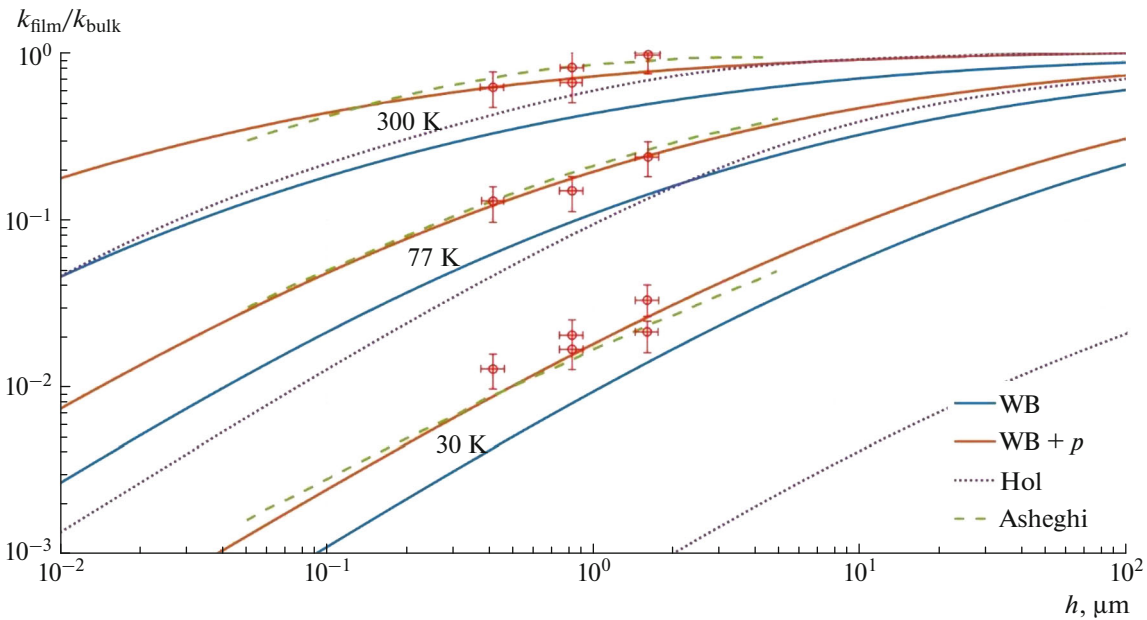


Fig. 6. Thermal conductivity of silicon films along the direction within a thickness range from 10 nm to 100 μm : WB is the model of the authors under the condition of diffuse reflection ($p = 0$); WB + p is the model of the authors for $p = 0.4, 0.5,$ and 0.8 for the temperature $T = 30, 70,$ and 300 K, respectively; Hol is the Holland model (4), (5) with $p = 0$. Asheghi is the model of thermal conductivity calculation [23] based on the rearrangement of the Boltzmann equation taking into account the size effect. Dots correspond to the experimental data [23].

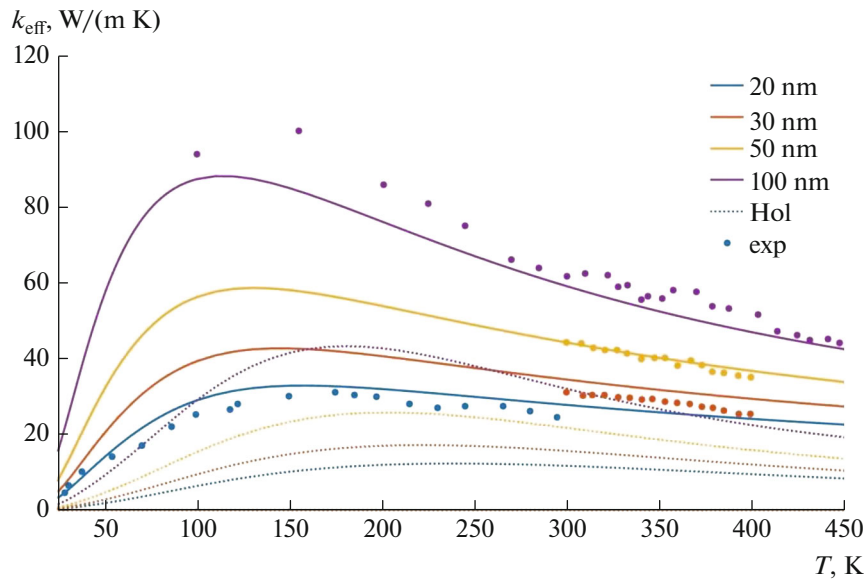


Fig. 7. Thermal conductivity of silicon films within a temperature range from 20 to 450 K: solid lines show the calculation by the updated model; dotted lines show the calculation by the Holland model (4), (5); dots correspond to experimental data from the following works: for 100 nm [24], for 30 and 50 nm [25], for 10 nm [26].

CONCLUSIONS

This work presents an updated model of the thermal conductivity calculation of silicon and germanium films within a wide range of temperatures and thicknesses. The model is based on the strict analysis

of the processes of phonon interaction and propagation. In the first place, the polynomial approximations of real dispersion curves are applied instead of linear approximations, which provides the possibility to strictly investigate the dynamics of phonons in the crystalline lattice. In the second place, the times of

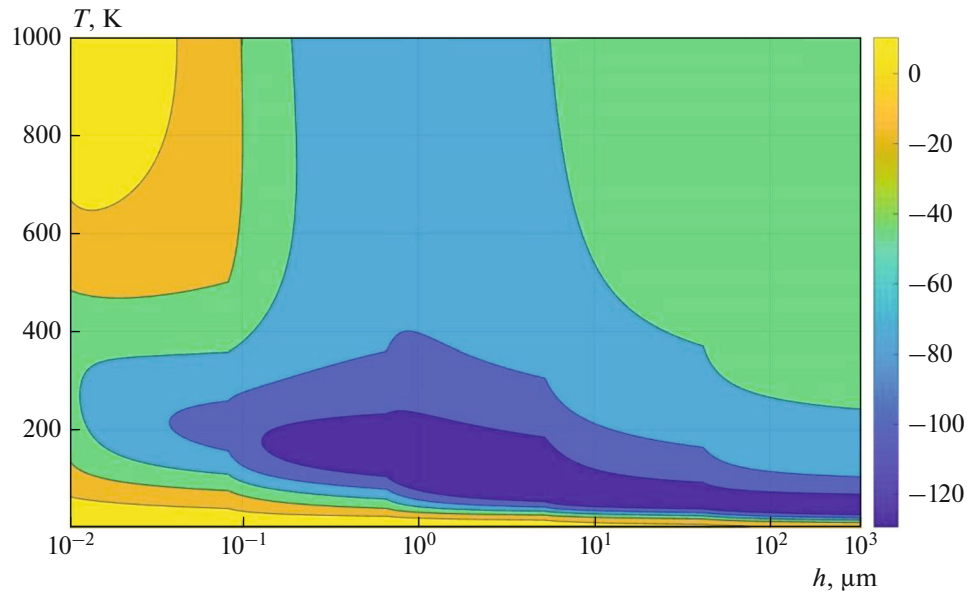


Fig. 8. Comparison of thermal conductivity by the Holland model and the updated model for silicon films.

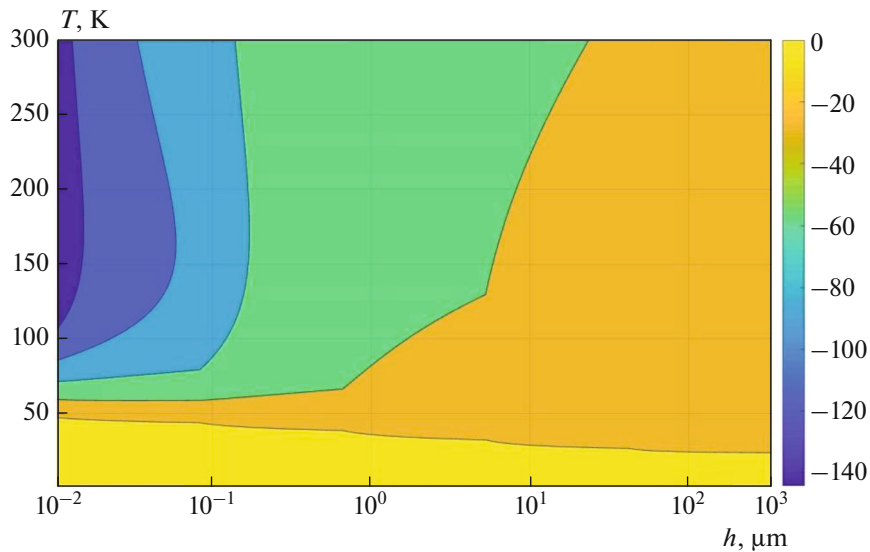


Fig. 9. Comparison of thermal conductivity using the linear law of dispersion and polynomial law (10) for silicon films.

phonon–phonon interactions derived on the basis of the modern method from the “first principles” are used, in which fitting parameters are absent.

The fundamental specific feature of the presented approach is its strong predictive ability, which distinguishes the method from models of Holland, Slack, etc., in which a high accuracy between the calculation and experiment is achieved by means of introducing fitting parameters. The detailed qualitative and quantitative comparison of the results of calculation by the

“classical” and “updated” models shows a good agreement of theory and experiment.

A weak point in the modern models is the absence of the correct technique for taking into account the phonon interaction with boundaries of the sample. This problem is especially urgent for structures of the micro- and nanoscale, in which the diffusion-ballistic and ballistic mechanisms of heat transfer are implemented. The further development of methods for thermal conductivity calculation for simulating new structures in advanced semiconductor (and not only)

devices is possible only by the way of specification of the time of scattering on the sample boundary.

FUNDING

This work was supported by the Ministry of Education and Science of the Russian Federation, project 16.8107.2017/6.7.

CONFLICT OF INTEREST

The authors declare that they have no conflicts of interest.

REFERENCES

1. A. A. Barinov, K. Chzhan, B. Lyu, and V. I. Khvesyuk, *Nauka Obrazov.*, No. 6, **56** (2017).
<https://doi.org/10.7463/0617.0001221>
2. E. Pop and K. E. Goodson, *J. Electron. Packag.* **128**, 102 (2006).
<https://doi.org/10.1115/1.2188950>
3. V. I. Khvesyuk, *Inzh. Zh.: Nauka Innov.*, No. 5 (17) (2013).
<https://doi.org/10.18698/2308-6033-2013-5-721>
4. V. I. Khvesyuk and A. S. Skryabin, *High Temp.* **55**, 428 (2017).
<https://doi.org/10.1134/S0018151X17030129>
5. A. A. Barinov, Zh. Tsao, and V. I. Khvesyuk, *Nauka Obraz.*, No. 05, 140 (2016).
<https://doi.org/10.7463/0516.0840329>
6. S. L. Shinde, G. P. Srivastava, and H. M. Tütüncü, *Length-Scale Dependent Phonon Interactions* (Springer, New York, 2014).
7. J. A. Reisland, *The Physics of Phonons* (Wiley, London, 1973).
8. A. Mittal and S. Mazumder, *J. Heat Transfer* **132**, 52402 (2010).
<https://doi.org/10.1115/1.4000447>
9. M. G. Holland, *Phys. Rev.* **132**, 2461 (1963).
<https://doi.org/10.1103/PhysRev.132.2461>
10. J. D. Chung, A. J. H. McGaughey, and M. Kaviani, *J. Heat Transfer* **126**, 376 (2004).
<https://doi.org/10.1115/1.1723469>
11. C. J. Glassbrenner and G. A. Slack, *Phys. Rev. A* **134**, 1058 (1964).
<https://doi.org/10.1103/PhysRev.134.A1058>
12. D. T. Morelli, J. P. Heremans, and G. A. Slack, *Phys. Rev. B* **66**, 195304 (2002).
<https://doi.org/10.1103/PhysRevB.66.195303>
13. P. G. Klemens, *Proc. Phys. Soc. A* **68**, 1113 (1955).
<https://doi.org/10.1088/0370-1298/68/12/303>
14. S. Tamura, *Phys. Rev. B* **27**, 858 (1983).
<https://doi.org/10.1103/PhysRevB.27.858>
15. H. B. G. Casimir, *Physica (Amsterdam, Neth.)* **5**, 495 (1938).
[https://doi.org/10.1016/S0031-8914\(38\)80162-2](https://doi.org/10.1016/S0031-8914(38)80162-2)
16. R. Berman, E. L. Foster, and J. M. Ziman, *Proc. R. Soc. London, Ser. A* **231** (1184), 130 (1955).
<https://doi.org/10.1098/rspa.1955.0161>
17. A. Ward and D. A. Broido, *Phys. Rev. B* **81**, 85205 (2010).
<https://doi.org/10.1103/PhysRevB.81.085205>
18. V. I. Khvesyuk and A. A. Barinov, *J. Phys.: Conf. Ser.* **891**, 012352 (2017).
<https://doi.org/10.1088/1742-6596/891/1/012352>
19. G. Dolling, in *Lattice Vibrations in Crystals with the Diamond Structure*, Vol. 2 of *Proceedings of the Symposium on Inelastic Scattering of Neutrons in Solids and Liquids* (IAEA, Vienna, 1963), p. 37.
[https://doi.org/10.1016/0029-5582\(62\)90477-7](https://doi.org/10.1016/0029-5582(62)90477-7)
20. G. Nilsson and G. Nelin, *Phys. Rev. B* **6**, 3777 (1972).
<https://doi.org/10.1103/PhysRevB.6.3777>
21. V. I. Ozhogin, A. V. Inyushkin, A. N. Taldenkov, A. V. Tikhomirov, G. E. Popov, E. Haller, and K. Itoh, *JETP Lett.* **63**, 490 (1996).
<https://doi.org/10.1134/1.567053>
22. C. J. Glassbrenner and G. A. Slack, *Phys. Rev. A* **134**, 1058 (1964).
<https://doi.org/10.1103/PhysRev.134.A1058>
23. M. Asheghi, Y. K. Leung, S. S. Wong, and K. E. Goodson, *Appl. Phys. Lett.* **71**, 1798 (1997).
<https://doi.org/10.1063/1.119402>
24. M. Asheghi and W. Liu, *J. Heat Transfer* **128**, 75 (2006).
<https://doi.org/10.1115/1.2130403>
25. M. Maldovan, *J. Appl. Phys.* **101**, 113110 (2012).
<https://doi.org/10.1063/1.4752234>
26. M. Asheghi and W. Liu, *Appl. Phys. Lett.* **84**, 3819 (2004).
<https://doi.org/10.1063/1.1741039>

Translated by M. Samokhina